

Bulk-boundary-transport correspondence of the second-order topological insulators

Yuxiong Long^{§,1}, Miaomiao Wei^{§,1}, Fuming Xu^{1,*} and Jian Wang^{1,2,3,†}

¹College of Physics and Optoelectronic Engineering, Shenzhen University, Shenzhen 518060, China

²Department of Physics, The University of Hong Kong, Pokfulam Road, Hong Kong, China

³Department of Physics, University of Science and Technology of China, Hefei, Anhui 230026, China

The bulk-boundary correspondence of the second-order topological insulator (SOTI) has been well established, but a universal transport signature for open systems is still absent. For a variety of SOTIs induced by applying in-plane magnetic fields in Z_2 -invariant first-order TIs, rotating this magnetic field features the spin pump mechanism while maintaining the SOTI phase. We demonstrate that, this spin pump can generate quantized pure spin current when tuning the magnetic field strength, which corresponds to the formation of topological corner states characterizing SOTI in two-dimensional (2D) systems. Quantized spin pump is discovered in various 2D and 3D SOTI models evolved from Z_2 -invariant TIs, which is robust against disorder and universally independent of system parameters including Fermi energy, system size, magnetic field strength, and pumping frequency. These findings suggest that this universal quantized spin pump can characterize the bulk-boundary-transport correspondence of SOTIs. Quantized spin pump can also be realized by combining pseudo spin such as the orbital degree of freedom with the rotating magnetic field, which could be achieved in higher-order photonic or acoustic topological systems. Such a quantized spin pump is promising as an accurate and stable single-spin source.

I. INTRODUCTION

Topological phases of matter have corresponding signatures in various spatial domains. For instance, Chern insulator is characterized by Chern number in bulk systems; when it is confined with boundaries, spinless edge states emerge; transport measurements show universal quantized Hall conductance in open systems^{1,2}. Such bulk-boundary-transport correspondence is also valid for topological insulators (TI, or quantum spin Hall (QSH) effect)³⁻⁷, which is represented by the Z_2 invariant, helical edge states, and universal quantized spin Hall conductance, respectively. Universal quantized transport signature is the manifestation of bulk topological invariants in open systems⁸⁻¹⁰.

For higher-order TIs, the bulk-boundary correspondence has been well established. The second-order TI (SOTI) is described by topological invariants including quadruple moment¹¹⁻¹³, Wannier center¹⁴, nested Wilson loop^{11,15,16}, Zak phase¹⁷, winding number^{18,19}, etc. Meanwhile, the boundary states of SOTI are characterized by 0-dimensional (0D) corner states in 2D systems and 1D hinge modes in 3D systems²⁰⁻²³. Topological corner states of SOTI are localized in real space and the corresponding energy levels are embedded in a large energy gap, which hardly contribute to transport. There are a few attempts on the resonant tunneling^{24,25} and charge pumping^{25,26} properties of topological corner states. However, as far as we know, universal quantized transport signature of SOTI is absent so far.

Thouless pump²⁷ can reveal the band topology and describe quantized charge pumping in bulk higher-order TIs^{28,29}, but not for open systems. On the other hand, quantum parametric pump^{30,31} generates nonzero charge current at zero bias voltages, by adiabatically manipulating system parameters such as gate voltage or magnetic field. It was shown that the pumped charge and current in parametric pump are closely related to Berry phase and Berry curvature³², which suggests that parametric pump could feature quantized transport of SOTI. Specifically, when the pump is realized by periodically ro-

tating the magnetic field, a spin pump is constructed, which induces pure dc spin current³³⁻³⁶.

A variety of second-order TIs are induced by applying in-plane magnetic fields in the Z_2 -invariant first-order TIs^{19,37-42}. The role of this magnetic field is breaking the time-reversal symmetry; its direction can be arbitrary and rotating this in-plane magnetic field does not affect the SOTI phase. Since the magnetic field usually couples with spin, it is natural to construct spin pump via rotating the in-plane magnetic field to investigate spin transport of open SOTI systems. Here an open system means attaching leads to the SOTI system to measure its transport properties.

In this work, we demonstrate that, for SOTIs evolved from the Z_2 -invariant TI by applying an in-plane magnetic field, integer spin quanta are pumped out per cycle when rotating this magnetic field, which gives rise to the quantization of spin transport. We show that, in finite/closed systems, the onset of quantization of spin current corresponds to formation of topological corner states representing SOTI, suggesting that quantized spin pump can serve as the quantized transport signature of SOTI that evolves from Z_2 -invariant TIs. Quantized spin current is discovered in various 2D and 3D SOTI systems including the Bernevig-Hughes-Zhang (BHZ) model^{37,40}, the Kane-Mele model¹⁹, and the pseudo spin model³⁷, where it is found to be robust against disorder and independent of system parameters such as Fermi energy, magnetic field strength and rotating frequency, and system size. Therefore, this quantized spin pump represents universal quantized transport signature and can be adopted to describe the bulk-boundary-transport correspondence of SOTIs.

II. SPIN PUMP VIA ROTATING MAGNETIC FIELD

We start with a 2D model system for spin pump, which is shown in Fig. 1(a). A rotating magnetic field is applied in the central region of this two-lead system, whose Hamiltonian

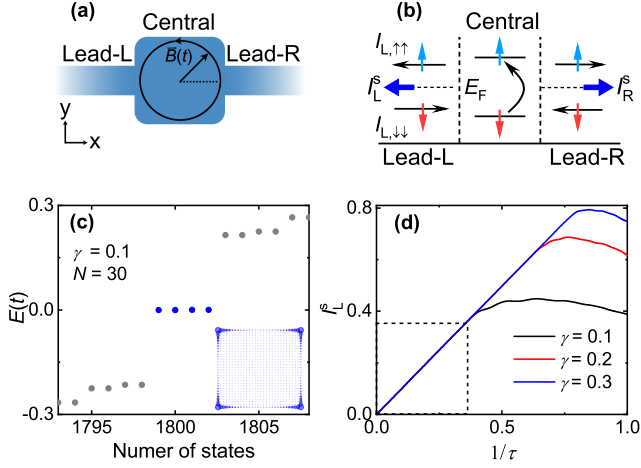


FIG. 1. (a) Schematic of a 2D spin pump setup. An in-plane rotating magnetic field is applied in the central region of a two-lead system with zero bias voltages. (b) Illustration of the spin pumping mechanism. (c) Energy levels for a $N \times N$ lattice of the BHZ model of SOTI. Zero energy levels (blue dots) corresponds to topological corner states which locates at the four corners of the square lattice shown in the inset. (d) Pumped spin current in the left lead as a function of the pumping frequency ($1/\tau = \omega/2\pi$) for different magnetic field strengths.

consists of three parts:

$$H = H_0 + H_{rot} + H_T. \quad (1)$$

H_0 is the Hamiltonian of the central region as well as the left and right leads, which is assumed to preserve time-reversal symmetry (TRS) and spin degeneracy. H_{rot} is the time-dependent Hamiltonian induced by the rotating magnetic field in the central region, which is typically defined as

$$H_{rot} = \sum_i \gamma_i \left[e^{-i\omega t} c_{i\uparrow}^\dagger c_{i\downarrow} + e^{i\omega t} c_{i\downarrow}^\dagger c_{i\uparrow} \right], \quad (2)$$

where $c_{i\uparrow}^\dagger$ ($c_{i\downarrow}$) is the creation (annihilation) operator for a spin-up (\uparrow) (spin-down \downarrow) electron at site i of the central region. γ_i is the magnetic field strength at site i , which is uniform in this work. ω is the rotating frequency, which determines the pumping period $\tau = 2\pi/\omega$. Clearly, H_{rot} reflects the spin flipping process through the coupling between the electron spin and the external magnetic field. H_T describes the coupling between the central region and two leads. The specific form of H_T depends on the Hamiltonians of the model system. Ref. [24] shows H_T for a 2D honeycomb lattice with nearest- and next-nearest-neighbor hoppings.

The spin pumping mechanism is shown in Fig. 1(b), where a spin-down electron is driven out of equilibrium by the rotating magnetic field and turned into a spin-up electron with higher energy through the spin flipping process. When periodically rotating the magnetic field, spin-down polarized currents continuously flow into the central region, and spin-up polarized currents flow out to both leads. If H_0 is spin conserved, charge currents cancel with each other and pure spin

currents are generated in the leads. Notice that both the magnitude and directions of the spin currents persist during the pumping period, which features constant dc spin currents. Since spin currents in both leads flow out or in simultaneously, this spin pump forms a unipolar spin battery^{36,43,44}.

The pumped spin-polarized current in lead α ($\alpha = L, R$) with spin σ is obtained by the nonequilibrium Green's function formalism ($\hbar = e = 1$)^{36,45}:

$$I_{\alpha,\sigma\sigma} = \int \frac{dE}{2\pi} (f(E) - f(E + \bar{\sigma}\omega)) \text{Tr} \left[G_{\sigma\bar{\sigma}}^r(E) \Gamma_{\sigma\bar{\sigma}}(E + \bar{\sigma}\omega) G_{\sigma\bar{\sigma}}^a(E) \Gamma_{\alpha,\sigma\sigma}(E) / 4\pi^2 \right], \quad (3)$$

where $f(E)$ is the Fermi distribution function with energy E . $\sigma/\bar{\sigma}$ labels spin polarization \uparrow/\downarrow in the z -direction and stands for ± 1 for the electron energy. Γ_α is the linewidth function of lead α , and $\Gamma = \sum_\alpha \Gamma_\alpha$. $G_{\sigma\bar{\sigma}}^{r(a)}$ is the retarded (advanced) nonequilibrium Green's function of the system. Its definition and the derivation of Eq. (3) are presented in the [Supporting Information](#). When the Hamiltonian H_0 is spin conserved, this spin pump generates pure spin current,

$$I_\alpha^s = \frac{1}{2} (I_{\alpha,\uparrow\uparrow} - I_{\alpha,\downarrow\downarrow}). \quad (4)$$

If H_0 is not spin conserved, only spin-polarized currents are pumped out. In the following, we investigate the spin pumping characteristics of various SOTI models.

III. THE BHZ MODEL OF SOTI

The BHZ model has been widely used for describing quantum spin Hall states of HgTe/CdTe quantum wells^{4,5} as well as topological surface states of 3D TI Bi₂Se₃^{6,7}. The BHZ model can also be generalized to investigate SOTI, which is achieved by introducing an in-plane magnetic field^{37,40}. When rotating this magnetic field to facilitate spin pump, the corresponding Hamiltonians read^{37,40}

$$H_0 = [-m + (t \cos k_x + t \cos k_y)] \tau_z \otimes \sigma_z + \lambda \sin k_x \tau_x \otimes \sigma_z - \lambda \sin k_y \tau_y \otimes \sigma_z,$$

$$H_{rot} = \gamma (\cos k_x - \cos k_y) \tau_0 \otimes (\sigma_x \cos \omega t + \sigma_y \sin \omega t),$$

where $\tau_{x/y/z}$ represent orbital degree of freedom, and $\sigma_{x/y/z}$ are Pauli matrices for spin. γ is the strength of the uniform magnetic field, which acts on in-plane spin $\sigma_{x/y}$. ω is the rotating frequency of the field and also serves as the pumping frequency. Other parameters of the model are conventionally defined in Refs.^{37,40}. Notice that H_0 preserves TRS and spin conservation of σ_z , while H_{rot} breaks TRS.

For a finite system, its zero energy levels and eigenfunction distribution are shown in Fig. 1(c). Four blue dots embedded in the large energy gap corresponds to the second-order topological corner states, whose eigenfunctions are localized at four corners of the square lattice. When rotating the magnetic field in a two-lead open system, pure spin currents are

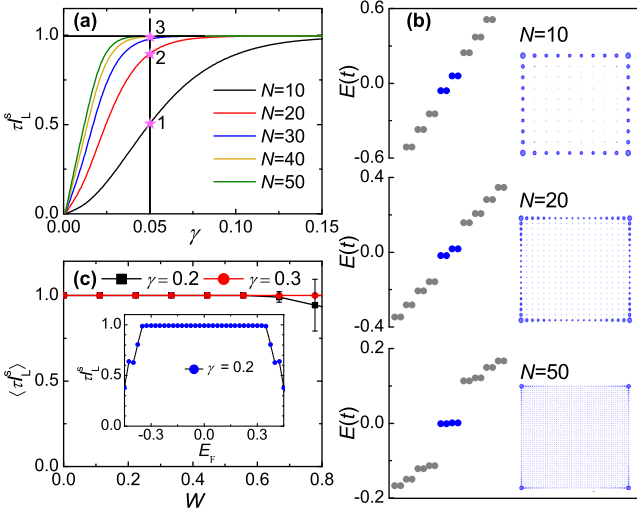


FIG. 2. (a) τI_L^s versus γ for different system sizes. (b) Energy levels near $E = 0$ (blue dots) and their eigenfunction distribution at $\gamma = 0.05$ for different system sizes $N = 10, 20$, and 50 , respectively. (c) Ensemble-averaged total spin current $\langle \tau I_L^s \rangle$ against disorder strength W . Error bar labels standard deviation. Inset shows τI_L^s versus the Fermi energy. $N = 20$ in panel (c).

generated. The pumped spin current in the left lead is plotted in Fig. 1(d), where I_L^s increases linearly with the pumping frequency in a large range ($1/\tau = \omega/2\pi$), regardless of the field strength. This observation suggests the existence of an adiabatic regime in which I_L^s can be scaled with the pumping frequency. From Eq. (3), when expanding the Fermi distribution function $f(E + \omega)$ to the first order in the pumping frequency ω , we have $f(E) - f(E + \omega) = -f'(E)\omega$. At zero temperature, $f'(E)$ is a δ -function, which leads to:

$$I_{\alpha,\sigma\sigma} = \frac{\omega}{2\pi} \text{Tr} [G_{\sigma\bar{\sigma}}^r(E)\Gamma_{\sigma\bar{\sigma}}(E)G_{\bar{\sigma}\sigma}^a(E)\Gamma_{\alpha,\sigma\sigma}(E)/4\pi^2].$$

This expression shows that $I_{\alpha,\sigma\sigma}$ scales linearly with ω in a certain range, where the scaled current $2\pi I_{\alpha,\sigma\sigma}/\omega = \tau I_{\alpha,\sigma\sigma}$ is a constant.

We further study the scaled current τI_L^s , which also represents the total spin current in one pumping period. τI_L^s as a function of the magnetic field strength is shown in Fig. 2(a). It is found that τI_L^s increases with the strength γ , and reaches a quantized plateau beyond a critical threshold γ_c . The threshold γ_c for quantized τI_L^s is smaller for larger system sizes. At a fixed γ , we plot the energy levels and corresponding eigenfunction distribution for several finite systems in Fig. 2(b), which are labeled by 1 to 3 in Fig. 2(a). For $N = 10$, $\tau I_L^s \approx 0.5$ is far from quantization; energy levels of the finite system are evenly separated; the eigenfunctions for near zero energy levels (blue dots) uniformly spread at the boundaries of the square lattice characterizing quantum spin Hall edge states. When $N = 20$, the scaled current increases to $\tau I_L^s \approx 0.9$; near zero energy levels (blue dots) deviate from other levels and the eigenfunction distribution is obviously more condense at four corners. For $N = 50$, τI_L^s is well quantized; zero energy levels are isolated in a large gap and

the eigenfunction forms localized topological corner states. The numerical evidence suggests that the onset of quantized spin current in open systems corresponds to the formation of topological corner states in confined/finite systems.

Disorder effect on the quantized spin current is also evaluated. Fig. 2(c) shows that the ensemble-averaged total spin current $\langle \tau I_L^s \rangle$ is robust against Anderson-type disorder in a large range of disorder strength. As an important parameter, the Fermi energy is scanned. In the inset of Fig. 2(c), $\tau I_L^s = 1$ is found in a large energy interval, which corresponds to the energy gap E_g of a finite system with the same size. Meanwhile, this energy range for $\tau I_L^s = 1$ coincides with the linear regime for I_L^s in Fig. 1(d), which establishes the relation $E_g \approx \hbar\omega_c$ with ω_c the cutoff pumping frequency of the linear regime. This is another evidence that links quantized spin current in open systems with the topological property of finite systems. All these results demonstrate that, the quantized spin current τI_L^s is universally independent of system parameters including the magnetic field strength, pumping frequency, system size, Fermi energy (within the topological energy gap), and robust against disorder, which represents a universal quantized transport signature of the BHZ model of SOTI.

The quantized spin current τI_L^s has clear physical meaning. Since I_L^s is pure spin current and τ is the pumping period, $\tau I_L^s = n$ corresponds to integer spin quanta pumped per cycle,

$$\tau I_L^s = \frac{2\pi}{\omega} I_L^s = \frac{2\pi}{\omega} [I_{L,\uparrow\uparrow} - I_{L,\downarrow\downarrow}] = n.$$

We have shown that τI_L^s is universally quantized to $n = 1$ for the BHZ model. Different from quantized charge conductance of Chern insulators and quantized spin-degenerate charge conductance of Z_2 -invariant TIs, quantized spin pump character-

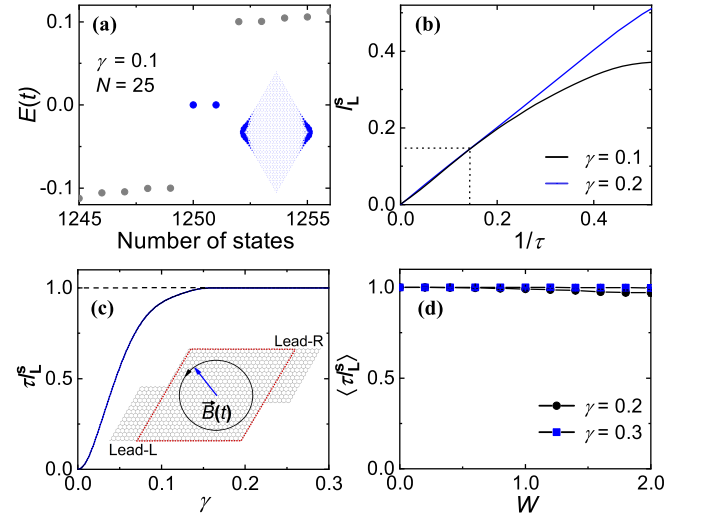


FIG. 3. (a) Zero energy levels and eigenfunction distribution of the Kane-Mele model of SOTI for a diamond-shaped honeycomb lattice. (b) Spin current as a function of the pumping frequency. (c) Total spin current per cycle versus the magnetic field strength. (d) Ensemble-averaged total spin current $\langle \tau I_L^s \rangle$ versus the disorder strength. $N = 25$ in all panels.

TABLE I. Summary of the symmetry, topological, and spin pump features for different models. '√' ('×') denotes the presence (absence) of the corresponding property.

Model	BHZ	Kane-Mele	Pseudo spin	MTI	Electric quadrupole insulator	3D model
TRS	√	√	√	×	√	√
First-order TI	Helical edge	Helical edge	Helical edge	Chiral edge	×	Helical surface
Second-order TI	Corner	Corner	Corner	Corner	Corner	Hinge states
Quantized spin pump	$n = 1$	$n = 1$	$n = 2$	×	×	$n = 2$

izes the universal transport signature of SOTI. It is reasonable since charge conductance is driven by electric field, while rotating magnetic field drives spin current. The validation of this quantized spin pump is further verified in other SOTI models, as shown below.

IV. THE KANE-MELE MODEL OF SOTI

The Kane-Mele model describes quantum spin Hall effect in 2D honeycomb lattice, such as graphene³ and silicene⁴⁶. Recently, Jacutingaite family materials (Pt₂HgSe₃ and Pd₂HgSe₃) have been proposed as promising Kane-Mele quantum spin Hall materials with a predicted topological gap up to 0.5 eV⁴⁷⁻⁵⁰. When introducing an in-plane magnetic field in the Kane-Mele model, SOTI emerges in 2D honeycomb lattice¹⁹. The Kane-Mele Hamiltonian is expressed as

$$H_0 = -t \sum_{\langle ij \rangle} c_i^\dagger \sigma_0 c_j + it_{\text{SO}} \sum_{\langle ij \rangle} \nu_{ij} c_i^\dagger \sigma_z c_j. \quad (5)$$

Here t is the nearest-neighbor hopping energy. t_{SO} is the strength of intrinsic spin-orbit coupling between next-nearest-neighbor sites. $\nu_{ij} = +1(-1)$ when an electron jumps from site j to site i by taking a clockwise (anticlockwise) turn. H_{rot} due to the rotating magnetic field is the same as Eq. (2).

The Kane-Mele model of SOTI is represented by a pair of topological corner states residing in a diamond-shape confined system, and the corresponding zero energy levels are inside a large gap, as shown in Fig. 3(a). Pumped spin current I_L^s of a two-lead system increases linearly with the pumping frequency in the region enclosed by dash lines in Fig. 3(b). We observe the relation $E_g \approx \hbar\omega_c$ again, where E_g is the band gap of the finite system and ω_c is the cutoff frequency of the linear pumping region. The total spin current τI_L^s per cycle increases with the magnetic field strength in Fig. 3(c), and quantizes to $n = 1$ when $\gamma > 0.15$. Fig. 3(d) demonstrates the robustness of quantized spin current against disorder. Other system parameters including system size and Fermi energy are also checked, which all support that spin current τI_L^s is universally quantized for the Kane-Mele model of SOTI.

V. DISCUSSION AND SUMMARY

The spin pump properties via rotating magnetic field for other SOTI models are also investigated, including the pseudo spin model³⁷, electric quadrupole insulator¹¹, magnetic topological insulator (MTI)⁵¹, and 3D model with topological

hinge states²¹. Although possessing different symmetries and first-order TI precursors, they all belong to the SOTI family. The main features are summarized in Table. I, and detailed numerical results are presented in the [Supporting Information](#).

Observations from Table. I are in order:

(1) SOTI is induced by the in-plane magnetic field in three types of systems, which are categorized into: (a) Z_2 -invariant first-order TI which has TRS; (b) electric quadrupole insulator (2D SSH chain) which maintains TRS; (c) magnetic topological insulator (MTI) that breaks TRS;

(2) Rotating the in-plane magnetic field pumps quantized spin current or integer spin quanta in SOTIs whose precursor is Z_2 -invariant first-order TI; for the pseudo spin model and the 3D model, the quantization number is $n = 2$ due to the degeneracy in the Hamiltonian; for electric quadrupole insulator and MTI, only spin-polarized charge currents can be generated;

(3) For the pseudo spin model and the 3D model of SOTI, the rotating magnetic field acts on pseudo spin, i.e., orbital degree of freedom, which shows that quantized pseudo spin pump is also accessible; in these two models, real spin σ_z is not conserved but pseudo spin τ_z is conserved in H_0 part of the system Hamiltonian; the rotating magnetic field is coupled to pseudo spin $\tau_{x/y}$ and manipulates the strength and phase of nearest-neighbor hoppings; details are shown in the [Supporting Information](#);

(4) The 3D model of SOTI has conducting 1D hinge states as the second-order topological phase; quantized spin pump can be realized by connecting 2D leads to the 3D central region, where the way of connecting leads to the central region can be arbitrary; details are shown in the [Supporting Information](#);

(5) The quantized spin pump is independent of system size, Fermi energy, magnetic field strength, pumping frequency, spatial dimensionality, and robust against disorder, showing a universal feature.

In conclusion, for SOTIs evolved from Z_2 -invariant TIs by applying an in-plane magnetic field to break time-reversal symmetry, quantized spin pump is achieved via rotating this magnetic field. The quantization of pumped spin current corresponds to the formation of topological corner states representing SOTI. Quantized spin pump is verified in various 2D and 3D SOTI models whose precursor is Z_2 -invariant TI, and it is robust against disorder and independent of system parameters. As the universal quantized transport signature, quantized spin pump characterizes the bulk-boundary-transport correspondence of SOTIs.

The existence of higher-order bulk-boundary correspon-

dence and 1D hinge modes has been experimentally confirmed in bismuth^{52,53}. It was shown both theoretically and experimentally that spin pumping mechanism via rotating magnetic field enhances the Gilbert damping in ferromagnetic film/normal metal bilayers³³⁻³⁵. Quantized spin pump can be realized by combining the SOTI states with the rotating magnetic field mechanism. We notice that higher-order topological phases are more easily fabricated in photonic crystals⁵⁴⁻⁵⁷ and acoustic materials⁵⁸⁻⁶¹. Specifically, it was found that acoustic higher-order topology can be generated from first-order with Zeeman-like fields⁶². Since the quantized spin pump is also achievable via manipulating the pseudo spin such as the orbital degree of freedom, we expect that this quantization phenomenon can be observed in the second-order photonic and acoustic systems.

In the application aspect, such a quantized spin pump based

on SOTI precisely pumps integer spin quanta. An optimal quantum parametric pump is noiseless^{63,64} and was predicted to pump quantized charge per pumping period^{65,66}. Based on 1D TI, Fu and Kane proposed a Z_2 adiabatic spin pump preserving TRS⁶⁷, which could pump nonquantized spin per cycle. Before the emergence of SOTI, X.-L. Qi et al suggested that, when applying an in-plane magnetic field on one particular edge of the QSH state, a fractional charge $e/2$ is confined on the magnetic domain wall and rotating this magnetic field would generate a quantized dc electric current⁶⁸. The universally quantized spin pump proposed in this work can serve as an accurate, stable, and robust single-spin source, which is on demand in quantum computing and quantum information.

This work is supported by the National Natural Science Foundation of China (Grants No. 12034014, No. 12174262, and No. 12147164).

* xufuming@szu.edu.cn

† jianwang@hku.hk

§ These authors contributed equally to this work.

- ¹ K. von Klitzing, G. Dorda, and M. Pepper, New Method for High-Accuracy Determination of the Fine-Structure Constant Based on Quantized Hall Resistance, *Phys. Rev. Lett.* **45**, 494 (1980).
- ² F. Overney, B. Jeanneret, B. Jeckelmann, B. M. Wood, and J. Schurr, The quantized Hall resistance: towards a primary standard of impedance, *Metrologia* **43**(5), 409 (2006).
- ³ C. L. Kane and E. J. Mele, Quantum spin Hall effect in graphene, *Phys. Rev. Lett.* **95**, 226801 (2005).
- ⁴ B. A. Bernevig, T. L. Hughes, and S.-C. Zhang, Quantum Spin Hall Effect and Topological Phase Transition in HgTe Quantum Wells, *Science* **314**, 1757 (2006).
- ⁵ M. König, S. Wiedmann, C. Brüne, A. Roth, H. Buhmann, L. W. Molenkamp, X.-L. Qi, and S.-C. Zhang, Quantum Spin Hall Insulator State in HgTe Quantum Wells, *Science* **318**, 766 (2007).
- ⁶ H. Zhang, C.-X. Liu, X.-L. Qi, X. Dai, Z. Fang, and S.-C. Zhang, Topological insulators in Bi₂Se₃, Bi₂Te₃ and Sb₂Te₃ with a single Dirac cone on the surface, *Nat. Phys.* **5**, 438 (2009).
- ⁷ Y. Zhang, K. He, C.-Z. Chang, C.-L. Song, L.-L. Wang, X. Chen, J.-F. Jia, Z. Fang, X. Dai, W.-Y. Shan, S.-Q. Shen, Q. Niu, X.-L. Qi, S.-C. Zhang, X.-C. Ma, and Q.-K. Xue, Crossover of the three-dimensional topological insulator Bi₂Se₃ to the two-dimensional limit, *Nat. Phys.* **6**, 584 (2010).
- ⁸ N. Nagaosa, J. Sinova, S. Onoda, A. H. MacDonald, and N. P. Ong, Anomalous Hall effect, *Rev. Mod. Phys.* **82**, 1539 (2010).
- ⁹ D. Xiao, M.-C. Chang, and Q. Niu, Berry phase effects on electronic properties, *Rev. Mod. Phys.* **82**, 1959 (2010).
- ¹⁰ X.-L. Qi and S.-C. Zhang, Topological insulators and superconductors, *Rev. Mod. Phys.* **83**, 1057 (2011).
- ¹¹ W. A. Benalcazar, B. A. Bernevig, and T. L. Hughes, Quantized electric multipole insulators, *Science* **357**, 61 (2017).
- ¹² C.-A. Li, B. Fu, Z.-A. Hu, J. Li, and S.-Q. Shen, Topological Phase Transitions in Disordered Electric Quadrupole Insulators, *Phys. Rev. Lett.* **125**, 166801 (2020).
- ¹³ Y. B. Yang, K. Li, L. M. Duan, and Y. Xu, Higher-order topological Anderson insulators, *Phys. Rev. B* **103**, 085408 (2021).
- ¹⁴ M. Ezawa, Minimal models for Wannier-type higher-order topological insulators and phosphorene, *Phys. Rev. B* **98**, 045125 (2018).
- ¹⁵ S. Franca, J. van den Brink, and I. C. Fulga, An anomalous higher-order topological insulator, *Phys. Rev. B* **98**, 201114(R) (2018).
- ¹⁶ B. Kang, K. Shiozaki, and G. Y. Cho, Many-body order parameters for multipoles in solids, *Phys. Rev. B* **100**, 245134 (2019).
- ¹⁷ F. Liu and K. Wakabayashi, Higher-order topology and fractional charge in monolayer graphene, *Phys. Rev. Research* **3**, 023121 (2021).
- ¹⁸ M. J. Park, Y. Kim, G. Y. Cho, and S.-B. Lee, Higher-Order Topological Insulator in Twisted Bilayer Graphene, *Phys. Rev. Lett.* **123**, 216803 (2019).
- ¹⁹ Y. Ren, Z. Qiao, and Q. Niu, Engineering Corner States from Two-Dimensional Topological Insulators, *Phys. Rev. Lett.* **124**, 166804 (2020).
- ²⁰ X.-L. Sheng, C. Chen, H. Liu, Z. Chen, Z.-M. Yu, Y. X. Zhao, and S. A. Yang, Two-Dimensional Second-Order Topological Insulator in Graphdiyne, *Phys. Rev. Lett.* **123**, 256402 (2019).
- ²¹ F. Schindler, A. M. Cook, M. G. Vergniory, Z. Wang, S. S. P. Parkin, B. A. Bernevig, and T. Neupert, Higher-order topological insulators, *Sci. Adv.* **4**, eaat0346 (2018).
- ²² Y.-R. Ding, D.-H. Xu, C.-Z. Chen, X. C. Xie, Hinged quantum spin Hall effect in antiferromagnetic topological insulators, *Phys. Rev. B* **101**, 041404 (2020).
- ²³ B. Xie, H.-X. Wang, X. Zhang, P. Zhan, J.-H. Jiang, M. Lu, and Y. Chen, Higher-order band topology, *Nat. Rev. Phys.* **3**, 520 (2021).
- ²⁴ K.-T. Wang, Y. Ren, F. Xu, Y. Wei, and J. Wang, Transport induced dimer state from topological corner states, *Sci. China-Phys. Mech. Astron.* **64**, 257811 (2021).
- ²⁵ K.-T. Wang, F. Xu, B. Wang, Y. Yu, and Y. Wei, Transport features of topological corner states in honeycomb lattice with multihollow structure, *Front. Phys.* **17**, 43501 (2022).
- ²⁶ B.-L. Wu, A.-M. Guo, Z.-Q. Zhang, and H. Jiang, Quantized charge-pumping in higher-order topological insulators, *Phys. Rev. B* **106**, 165401 (2022).
- ²⁷ D. J. Thouless, Quantization of particle transport, *Phys. Rev. B* **27**, 6083 (1983).
- ²⁸ J. F. Wienand, F. Horn, M. Aidelsburger, J. Bibo, and F. Grusdt, Thouless Pumps and Bulk-Boundary Correspondence in Higher-Order Symmetry-Protected Topological Phases, *Phys. Rev. Lett.* **128**, 246602 (2022).
- ²⁹ R. Citro and M. Aidelsburger, Thouless pumping and topology, *Nat. Rev. Phys.* **5**, 87 (2023).
- ³⁰ M. Büttiker, A. Prêtre, and H. Thomas, Current partition in multiprobe conductors in the presence of slowly oscillating external

- potentials, *Z. Phys. B: Condens. Matter* **94**, 133 (1994).
- ³¹ P. W. Brouwer, Scattering approach to parametric pumping, *Phys. Rev. B* **58**, R10135 (1998).
 - ³² J. E. Avron, A. Elgart, G. M. Graf, and L. Sadun, Geometry, statistics, and asymptotics of quantum pumps, *Phys. Rev. B* **62**, R10618 (2000).
 - ³³ R. Urban, G. Woltersdorf, and B. Heinrich, Gilbert Damping in Single and Multilayer Ultrathin Films: Role of Interfaces in Non-local Spin Dynamics, *Phys. Rev. Lett.* **87**, 217204 (2001).
 - ³⁴ Y. Tserkovnyak, A. Brataas, and G.E.W. Bauer, Enhanced Gilbert Damping in Thin Ferromagnetic Films, *Phys. Rev. Lett.* **88**, 117601 (2002).
 - ³⁵ Y. Tserkovnyak, A. Brataas, and G.E.W. Bauer, Spin pumping and magnetization dynamics in metallic multilayers, *Phys. Rev. B* **66**, 224403 (2002).
 - ³⁶ B. Wang, J. Wang, and H. Guo, Quantum spin field effect transistor, *Phys. Rev. B* **67**, 092408 (2003).
 - ³⁷ Z. Song, Z. Fang, and C. Fang, ($d - 2$)-dimensional edge states of rotation symmetry protected topological states, *Phys. Rev. Lett.* **119**, 246402 (2017).
 - ³⁸ M. Ezawa, Topological Switch between Second-Order Topological Insulators and Topological Crystalline Insulators, *Phys. Rev. Lett.* **121**, 116801 (2018).
 - ³⁹ C. Chen, Z. Song, J.-Z. Zhao, Z. Chen, Z.-M. Yu, X.-L. Sheng, and S. A. Yang, Universal Approach to Magnetic Second-Order Topological Insulator, *Phys. Rev. Lett.* **125**, 056402 (2020).
 - ⁴⁰ Y. S. Hu, Y. R. Ding, J. Zhang, Z. Q. Zhang and C. Z. Chen, Disorder and phase diagrams of higher-order topological insulators, *Phys. Rev. B*, **104**, 094201 (2021).
 - ⁴¹ R. Chen, T. Liu, C. M. Wang, H.-Z. Lu, and X. C. Xie, Field-Tunable One-Sided Higher-Order Topological Hinge States in Dirac Semimetals, *Phys. Rev. Lett.* **127**, 066801 (2021).
 - ⁴² J. Zeng, C. Chen, Y. Ren, Z. Liu, W. Ren and Z. Qiao, Topological corner states in graphene by bulk and edge engineering, *Phys. Rev. B* **106**, L201407 (2022).
 - ⁴³ A. Brataas, Y. Tserkovnyak, G. E. W. Bauer, and B. I. Halperin, Spin battery operated by ferromagnetic resonance, *Phys. Rev. B* **66**, 060404(R) (2002).
 - ⁴⁴ Q.-f. Sun, H. Guo, and J. Wang, A Spin Cell for Spin Current, *Phys. Rev. Lett.* **90**, 258301 (2003).
 - ⁴⁵ W. Zheng, J. Wu, B. Wang, J. Wang, Q. Sun, and H. Guo, Parametric Quantum Spin Pump, *Phys. Rev. B* **68**, 113306 (2003).
 - ⁴⁶ C.-C. Liu, W. Feng, and Y. Yao, Quantum Spin Hall Effect in Silicene and Two-Dimensional Germanium, *Phys. Rev. Lett.* **107**, 076802 (2011).
 - ⁴⁷ A. Marrazzo, M. Gibertini, D. Campi, N. Mounet, and N. Marzari, Prediction of a Large-Gap and Switchable Kane-Mele Quantum Spin Hall Insulator, *Phys. Rev. Lett.* **120**, 117701 (2018).
 - ⁴⁸ I. Cucchi, A. Marrazzo, E. Cappelli, S. Riccò, F. Y. Bruno, S. Lisi, M. Hoesch, T. K. Kim, C. Cacho, C. Besnard, E. Giannini, N. Marzari, M. Gibertini, F. Baumberger, and A. Tamai, Bulk and Surface Electronic Structure of the Dual-Topology Semimetal Pt_2HgSe_3 , *Phys. Rev. Lett.* **124**, 106402 (2020).
 - ⁴⁹ K. Kandrai, P. Vancsó, G. Kukucska, J. Koltai, G. Baranka, Á. Hoffmann, Á. Pekker, K. Kamarás, Z. E. Horváth, A. Vymazalová, L. Tapasztó, and P. Nemes-Incze, Signature of Large-Gap Quantum Spin Hall State in the Layered Mineral Jacutingaite, *Nano Lett.* **20**, 5207 (2020).
 - ⁵⁰ M. Ur Rehman, M. Kiani, and J. Wang, Jacutingaite family: An efficient platform for coexistence of spin valley Hall effects, valley spin-valve realization, and layer spin crossover, *Phys. Rev. B* **105**, 195439 (2022).
 - ⁵¹ M. Ezawa, Magnetic second-order topological insulators and semimetals, *Phys. Rev. B* **97**, 155305 (2018).
 - ⁵² F. Schindler, Z. Wang, M. G. Vergniory, A. M. Cook, A. Murani, S. Sengupta, A. Yu. Kasumov, R. Deblock, S. Jeon, I. Drozdov, H. Bouchiat, S. Guéron, A. Yazdani, B. A. Bernevig, and T. Neupert, Higher-order Topology in Bismuth, *Nat. Phys.* **14**, 918 (2018).
 - ⁵³ L. Aggarwal, P. Zhu, T. L. Hughes, and V. Madhavan, Evidence for higher order topology in Bi and $\text{Bi}_{0.92}\text{Sb}_{0.08}$, *Nat. Comm.* **12**, 4420 (2021).
 - ⁵⁴ X.-D. Chen, W.-M. Deng, F.-L. Shi, F.-L. Zhao, M. Chen, and J.-W. Dong, Direct Observation of Corner States in Second-Order Topological Photonic Crystal Slabs, *Phys. Rev. Lett.* **122**, 233902 (2019).
 - ⁵⁵ B.-Y. Xie, G.-X. Su, H.-F. Wang, H. Su, X.-P. Shen, P. Zhan, M.-H. Lu, Z.-L. Wang, and Y.-F. Chen, Visualization of Higher-Order Topological Insulating Phases in Two-Dimensional Dielectric Photonic Crystals, *Phys. Rev. Lett.* **122**, 233903 (2019).
 - ⁵⁶ M. Li, D. Zhirihin, M. Gorbach, X. Ni, D. Filonov, A. Slobozhanyuk, Andrea Alù, and A. B. Khanikaev, Higher-order topological states in photonic kagome crystals with long-range interactions, *Nat. Photonics* **14**, 89 (2020).
 - ⁵⁷ M. Kim, Z. Jacob, and J. Rho, Recent advances in 2D, 3D and higher-order topological photonics, *Light-Sci. Appl.* **9**, 130 (2020).
 - ⁵⁸ H. Xue, Y. Yang, F. Gao, Y. Chong, and B. Zhang, Acoustic higher-order topological insulator on a kagome lattice, *Nat. Mater.* **18**, 108 (2019).
 - ⁵⁹ Q. Wei, X. Zhang, W. Deng, J. Lu, X. Huang, M. Yan, G. Chen, Z. Liu, and S. Jia, Higher-order topological semimetal in acoustic crystals, *Nat. Mater.* **20**, 812 (2021).
 - ⁶⁰ J. Du, T. Li, X. Fan, Q. Zhang, and C. Qiu, Acoustic Realization of Surface-Obstructed Topological Insulators, *Phys. Rev. Lett.* **128**, 224301 (2022).
 - ⁶¹ Z. Pu, H. He, L. Luo, Q. Ma, L. Ye, M. Ke, and Z. Liu, Acoustic Higher-Order Weyl Semimetal with Bound Hinge States in the Continuum, *Phys. Rev. Lett.* **130**, 116103 (2023).
 - ⁶² X. Huang, J. Lu, Z. Yan, M. Yan, W. Deng, G. Chen, and Z. Liu, Acoustic higher-order topology derived from first-order with built-in Zeeman-like fields, *Science Bulletin* **67**, 488 (2022).
 - ⁶³ J. E. Avron, A. Elgart, G. M. Graf, and L. Sadun, Optimal Quantum Pumps, *Phys. Rev. Lett.* **87**, 236601 (2001).
 - ⁶⁴ B. Wang and J. Wang, Optimal quantum pump in the presence of a superconducting lead, *Phys. Rev. B* **66**, 201305(R) (2002).
 - ⁶⁵ Y. Levinson, O. Entin-Wohlman, and P. Wölfle, Pumping at resonant transmission and transferred charge quantization, *Physica A* **302**, 335 (2001).
 - ⁶⁶ J. Wang and B. Wang, Quantization of adiabatic pumped charge in the presence of superconducting lead, *Phys. Rev. B* **65**, 153311 (2002).
 - ⁶⁷ L. Fu and C. L. Kane, Time reversal polarization and a \mathbb{Z}_2 adiabatic spin pump, *Phys. Rev. B* **74**, 195312 (2006).
 - ⁶⁸ X.-L. Qi, T. L. Hughes, and S.-C. Zhang, Fractional charge and quantized current in the quantum spin Hall state, *Nat. Phys.* **4**, 278 (2008).